

Evaluation of Transmission Channel Models Based on Simulations and Measurements in Real Channels

Emil Dumic,^{1,*} Gordan Sisul¹ and Sonja Grgic¹

¹ University of Zagreb, Faculty of Electrical Engineering and Computing, Department of Wireless Communications, Croatia

Abstract. This paper presents simulation environment that includes transmission channel models from the ETSI standard EN 300 744 (DVB-T system) and channel models based on real measured parameters. Our simulation includes transmitter and receiver, supports different system parameters (modulation, code rate, guard interval) and channel models. It is adaptive and reconfigurable environment that allows incorporation of hardware generated channel matrix in channel model and provides accurate estimation of system constraints. The model offers evaluation of channel models and can be used for testing and educational purposes.

Keywords. DVB-T, channel estimation, Gaussian channel, Ricean channel, Rayleigh channel, carrier-to-noise ratio.

PACS® (2010). 84.40.Ua, 89.70.Kn, 89.20.Ff.

1 Introduction

The reception conditions in communication system can, ideally, be described by the Gaussian channel which is based on direct signal path from transmitter to receiver [1]. In this channel impairment is caused by additive white Gaussian noise (AWGN) which is mainly produced by receiver itself. In addition to AWGN, Ricean channel takes into account the effect of multipath signals (echoes). The Ricean channel includes one direct signal path and additional indirect paths. The statistics of these multipath signals are approximated by Ricean distribution [2]. The third type of channel in DVB-T is Rayleigh channel with the distribution of echoes that corresponds to Rayleigh distribution. This channel includes only signals from indirect paths. When the delay time of echoes exceeds a certain value, multipath signals cause an increase in intersymbol interference

(ISI) which results in an increase in the bit-error rate. The increase of ISI can be corrected by increasing the transmission power.

In this paper different channel model are evaluated using model of DVB-T system and measurement results achieved in real DVB-T system. DVB-T is an abbreviation for Digital Video Broadcasting – Terrestrial; it is the DVB European-based consortium standard for the broadcast transmission of digital terrestrial television [3]. This system transmits compressed digital audio, video and other data in an MPEG transport stream [4, 5], using Coded Orthogonal Frequency Division Multiplexing (COFDM) modulation [6]. Rather than carrying the data on a single radio frequency (RF) carrier, OFDM works by splitting the digital data stream into a large number of slower digital streams, each of which digitally modulate a set of closely spaced adjacent carrier frequencies. In the case of DVB-T, there are two choices for the number of carriers known as 2K-mode or 8K-mode (4K-mode is rarely used) [3, 6].

The power requirements for DVB-T system can be determined using simulation that includes mathematical model to describe the channel characteristics. Results of simulation depend very much on channel description. The results of simulation are usually given in the terms of carrier-to-noise (C/N) ratio required for quasi-error free (QEF) reception. Different channel models result in different required transmission power to compensate the effect of echoes. Therefore, the accuracy of channel model is extremely important in simulation. The goal of our work was to develop simulation model for DVB-T system that incorporates real channel characteristics achieved through real measurements. Developed model provides simple but accurate evaluation of DVB-T system parameters.

Some other authors have already designed DVB-T simulation for Gaussian channel [7]. Others have shown that the minimum C/N values for good-quality portable DVB-T reception in a static Rayleigh channel – as given in the ETSI DVB-T standard – are too low. Therefore a new set of C/N values for portable urban reception was proposed [8].

This paper is organized as follows. Section 2 describes DVB-T transmitter and Section 3 describes DVB-T receiver. Section 4 presents simulation model. Section 5 presents simulation results and section 6 draws the conclusions.

* **Corresponding author:** Emil Dumic, University of Zagreb, Faculty of Electrical Engineering and Computing, Department of Wireless Communications, Croatia; E-mail: emil.dumic@fer.hr.

Received: July 19, 2011.

2 Technical Description of a DVB-T Transmitter

DVB-T transmitter, Figure 1, consists of several signal processing blocks [3]:

- Source coding and MPEG-2 multiplexing;
- Splitter;
- Multiplex adaptation and energy dispersal;
- External encoder (RS encoder);
- External interleaver (Convolutional interleaver, $I = 12$);
- Internal encoder (Punctured Convolutional Code);
- Internal interleaver;
- Mapper (+ pilots and Transmission Parameter Signaling (TPS) carriers);
- OFDM Transmitter and Guard Interval Insertion;
- DAC (digital to analogue converter) and front-end.

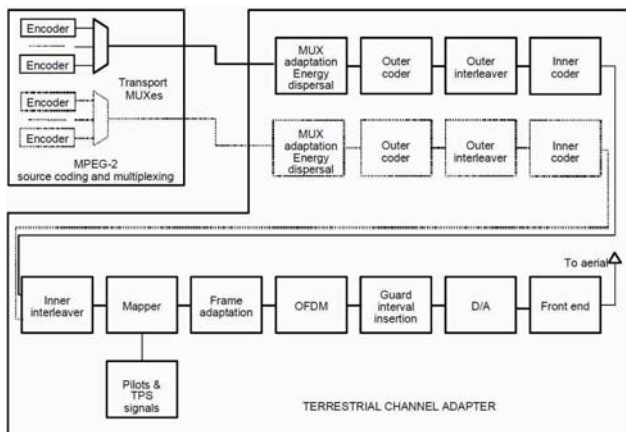


Figure 1. DVB-T transmitter block diagram.

2.1 Source Coding and MPEG-2 Multiplexing

Compressed video, audio and private data streams form elementary streams. Standards for video and audio compression in DVB-T system are [5]:

- video compression – MPEG-2, H.264/AVC and VC-1 [9–11];
- audio compression – MPEG-1 or MPEG-2 layer 2 backward compatible audio, AC-3 audio, Enhanced AC-3 audio, DTS audio or MPEG-4 AAC audio [12–14].

Elementary streams are firstly cut into packetized elementary streams (PES) and afterwards multiplexed into MPEG-2 transport stream (MPEG-2 TS), [2]. Each TS packet is 188 bytes long and can contain data from only one PES packet. MPEG-2 transport stream is primarily intended for the transport of TV programs over long distances via transmission supports or in environments susceptible to the introduction of relatively high error rates (BER, bit error rate, higher than 10^{-4}). There also exist MPEG-2 program stream (MPEG-2 PS), which is primarily intended for applications where the transmission channel or storage medium is supposed to introduce only a very low number of errors (BER $< 10^{-10}$).

2.2 Splitter

DVB-T includes the option of hierarchical modes allowing carrying streams with different priorities corresponding to different degrees of robustness. Constellation diagram can have a greater distance between adjacent states located in different quadrants than between adjacent states belonging to the same quadrant. Non-uniform constellations are defined by a parameter that can take three values ($\alpha = 1, 2, \text{ or } 4$), which define the distance between the sub-constellations of each quadrant ($\alpha = 1$ denotes same constellation as uniform, used in non-hierarchical transmission). In such a way two different bit streams can be transmitted, one bit stream modulating two the most significant bits (MSB) and other remaining bits (2 or 4, depending if it is 16-QAM or 64-QAM). The first bit stream can be then noisy QPSK and it is used for lower C/N ratio. The second bit stream can operate on higher bitrates, but it is more sensitive to channel errors. For example, the same channel can be broadcasted in SDTV and HDTV and the receiver uses the one depending on receiving conditions. It will be further discussed under “Mapper” subsection. In this paper we will describe and test only non-hierarchical mode.

2.3 Multiplex Adaptation and Energy Dispersal

DVB requires that energy dispersal should be undertaken before the correction process in order to obtain an evenly distributed energy within the RF channel. In order to avoid long series of 0's or 1's, which would bring DC content to the signal, the signal has to be randomized in order to ensure the energy dispersal in the channel. This is obtained by scrambling the signal by means of a pseudo-random binary sequence (PRBS) with the generator polynomial $1 + X^{14} + X^{15}$ [3]. The PRBS disperses the data but not the sync words (0x47) of the TS packets. The sync word is the first byte of each TS packet. The polynomial has a length of 1503 bytes. This exactly corresponds to eight TS packets minus the bitwise inverted sync word of the first TS packet. The generator is reinitialized by loading its regis-

ter with the sequence 100101010000000. Energy dispersal ensures a constant average modulator output level.

2.4 External Encoder

The outer coding is a Reed–Solomon coding. RS (204, 188, $T = 8$) code is used which is a shortened version of the code RS (255, 239, $T = 8$). It adds 16 parity bytes after the information bytes of the transport packets, which therefore become 204 bytes long. It can correct up to 8 erroneous bytes per packet. It is interesting to note that the input BER required for the RS code (as specified in the DVB-T specification to attain the so-called quasi-error-free channel with BER of 10^{-11}) is 2×10^{-4} . So, on average, this RS code should correct 20 million errors for each error it fails to correct ($2 \cdot 10^{-4} / 10^{-11} = 20\,000\,000$).

2.5 External Interleaver

Transmission errors corrupt not only a single bit but many bits following it in the data stream. A convolutional interleaver rearranges the transmitted packets with the purpose to increase the efficiency of the Reed–Solomon decoding by spreading the burst errors introduced by the channel over a longer time. External interleaver inserts 11 bytes from other TS packets between bytes from the same TS packet (at the input). This allows burst errors of maximum $12 \times 8 = 96$ bytes to be corrected because only eight or fewer errored bytes per TS packet are obtained after the deinterleaver in the DVB receiver/decoder.

2.6 Internal Encoder

Internal encoder uses convolutional coding and is an efficient complement to the Reed–Solomon coder and external interleaver. It is based on a mother convolutional code of rate 1/2 with 64 states (generator polynomials of the mother code are $G_1 = 171_{\text{OCT}}$ for X output and $G_2 = 133_{\text{OCT}}$ for Y output). Afterwards, puncturing the output of the convolutional encoder lowers the redundancy of the mother code. System shall allow code rates of 2/3, 3/4, 5/6 and 7/8, which involves not taking all successive bits of the two X and Y output bit streams, but only one of the two simultaneous bits with a certain puncturing ratio.

2.7 Internal Interleaver

Two separate interleaving processes are used to reduce the influence of burst errors, one operating on bits (bit interleaver) and another on groups of bits (symbol interleaver).

Depending on the modulation mode – QPSK, 16-QAM or 64-QAM – the bit interleaver comprises two, four or six paths. An input stream is demultiplexed into v sub-streams, where $v = 2$ for QPSK, $v = 4$ for 16-QAM, and $v = 6$ for 64-QAM.

Two modes are defined for the COFDM multicarrier method: 2K with 1705 carriers and 8K with 6817 carriers. The purpose of the symbol interleaver is to map v bit words onto the useful 1512 (2K mode) or 6048 (8K mode) active carriers per OFDM symbol. The interleaver output data words are grouped in 12 blocks of 126 bits in 2K mode and in 48 blocks of 126 bits in 8K mode. The symbol interleaver processes the bit groups to generate COFDM symbols. In our presentation, we will be focused mainly on 8K transmission, which is used in Croatia.

The symbol interleaver already allows insertion of scattered pilots, continual pilots and transmission parameter signaling (TPS) carriers at defined points of the COFDM symbol (it leaves these positions free).

2.8 Mapper

The system uses OFDM transmission. All data carriers in one OFDM frame are modulated using QPSK, 16-QAM, 64-QAM, non-uniform 16-QAM or non-uniform 64-QAM constellations. 68 consecutive symbols form one OFDM frame and 4 frames form OFDM super-frame.

Non-hierarchical transmission uses only uniform constellations. Hierarchical mode can use all above mentioned modulations. In the mapping block, assignment of the I/Q value pair takes place, Figure 2. The distance of the clouds of I/Q value pairs from the I and Q axes is determined by the parameter α , which may take the value 1, 2 or 4. So, $\alpha = 1$ is permissible in non-hierarchical modulation.

Hierarchical modulation is possible only with 16-QAM or 64-QAM in the DVB-T system and can use all α values. With 64-QAM, two of the six bits of each I/Q value pair are used for the high-priority path and the remaining four bits for the low-priority path. With 16-QAM, two out of four bits are allocated to each path.

701 scattered and continual pilot signals, modulated with BPSK with boosted power level amplitude (boosted by the factor 16/9), are added between useful pilots. Scattered pilots change places in every symbol, and every 4th symbol they repeat their place. Continual pilots have static places in every symbol. PRBS with the generator polynomial $1 + X^2 + X^{11}$ is added on these pilots, initialized with 1111111111.

68 TPS (Transmission Parameter Signals) bits are also sent between useful carriers. TPS are DBPSK modulated and indicate:

- modulation type (including α value);
- hierarchy information;
- guard interval;
- inner code rates;
- transmission mode (2K or 8K);
- frame number in a super-frame;
- cell identification.

QPSK		16-QAM			
Q		Q			
10	00	1000	1010	0010	0000
	I	1001	1011	0011	0001
11	01	1101	1111	0111	0101
		1100	1110	0110	0100

64-QAM							
Q							
100000	100010	101010	101000	001000	001010	000010	000000
100001	100011	101011	101001	001001	001011	000011	000001
100101	100111	101111	101101	001101	001111	000111	000101
100100	100110	101110	101100	001100	001110	000110	000100
110100	110110	111110	111100	011100	011110	010110	010100
110101	110111	111111	111101	011101	011111	010111	010101
110001	110011	111011	111001	011001	011011	010011	010001
110000	110010	111010	111000	011000	011010	010010	010000

Figure 2. QPSK, 16-QAM and 64-QAM mapping (non-hierarchical).

TPS carriers are only modulated along the I axis and so are a direct indication of the phase. TPS are defined over 1 OFDM frame (68 different bits), where in each OFDM symbol all 68 TPS pilots carry the same bit. TPS data is only used in special cases, such as changes in the parameters, resynchronizations, because the receiver must be able to synchronize, equalize, and decode the signal to gain access to the information held by the TPS pilots.

2.9 OFDM Transmitter and Guard Interval Insertion

OFDM modulation consists of N closely spaced orthogonal carriers of duration T_0 (each one is modulated with a conventional modulation scheme like QPSK, n -QAM or n -PSK), with a spacing of $1/T_0$ between two consecutive carriers. Increasing the number of carriers does not modify the payload bit rate, which remains constant. In DVB-T OFDM uses 2048 or 8192 carriers (2K and 8K mode).

Every OFDM block is extended, prefixing the end of the block to the beginning (cyclic prefix). The cyclic prefix serves as a guard interval and eliminates the intersymbol interference from the previous symbol. Insertion of the guard interval extends symbol duration by $1/4$, $1/8$, $1/16$ or $1/32$ to give the total symbol duration T_S . By the end of the guard interval, all echoes caused by multipath reception, reception of other transmitters in the SFN (SFN, Single Frequency Network) or Doppler effects in mobile reception, i.e. all fading effects, must have settled or decayed. The time signal of

length T_S , still digital, is applied to the digital-to-analogue converter (DAC).

2.10 DAC and Front-end

Digital signal is transformed into an analogue signal, with a DAC and then modulated to radio frequency (VHF, UHF) by the RF front-end. The occupied bandwidth is designed to accommodate DVB-T signal into 5, 6, 7, or 8 MHz channels. The base band sample rate provided at the DAC input depends on the channel width: it is $f_s = \frac{8}{7} \cdot B$ samples/s, where B is the channel width in Hz. In our paper we did not realize DAC, instead digital signal is itself transferred through channel

3 Technical Description of a DVB-T Receiver

DVB-T receiver consists of below described signal processing blocks:

- Front-end and ADC;
- Time and frequency synchronization;
- Guard interval disposal and OFDM Receiver;
- Channel Estimator and Channel Compensation;
- Demapper;
- Inner Deinterleaver;
- Internal Decoding (Viterbi Decoder);
- External Deinterleaving (Convolutional Deinterleaver $I = 12$);
- External decoding (RS Decoder);
- MUX adaptation;
- MPEG-2 demultiplexing and source decoding.

The receiving STB (Set-Top Box) adopts techniques which are dual to those ones used in the transmission. Its practical performance depends on hardware construction (it is not standardized like encoder).

4 Simulation Description

Simulation in our presentation covers main DVB-T processing blocks described in Section 2 and 3, Figure 3. It is made in Simulink, integrated in Matlab. Simulink is an environment for multidomain simulation and Model-Based Design for dynamic and embedded systems. Simulation is based on implemented DVB-T simulation in Matlab (command 'commdvbt') with fixed parameters (2K-mode, 64-QAM, FEC 3/4).

Simulation input is 188 bytes long random binary sequence (as it should be similar to 188 transport stream

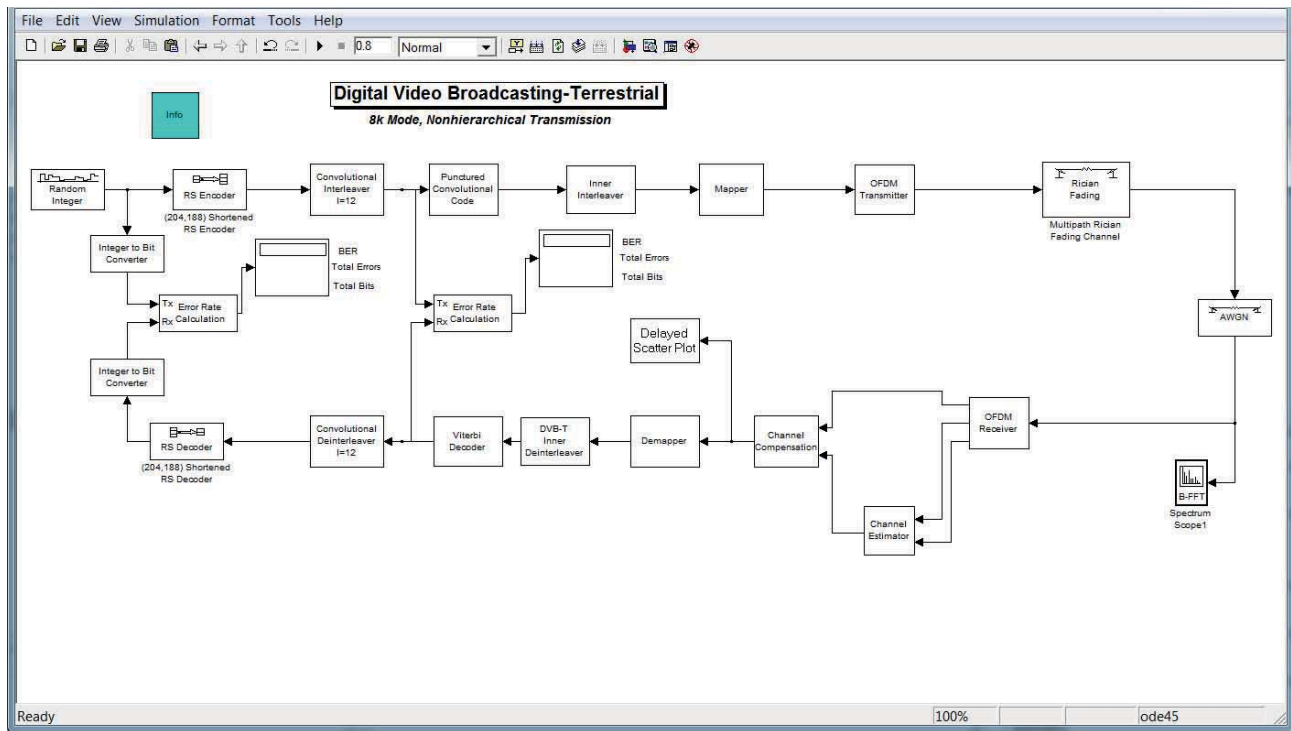


Figure 3. Main simulation model.

bytes after energy dispersal). Simulation works in 8k mode (which is used in Croatian DVB-T system). Different parameters can be chosen prior opening simulink model:

- modulation type ($\alpha = 1$): QPSK, 16-QAM or 64-QAM;
- FEC: 1/2, 2/3, 3/4, 5/6, 7/8;
- Guard interval: 1/4, 1/8, 1/16, 1/32.

Figure 3 shows main model after choosing above mentioned parameters. Simulation also shows constellation diagram (Figure 4). Additionally, bandlimited impulse response of the Rician (or Rayleigh) fading channel can also be shown, but it slows simulation down (Figure 5). Finally, BER is calculated, after internal decoding (Viterbi decoder) and external decoding (RS decoder).

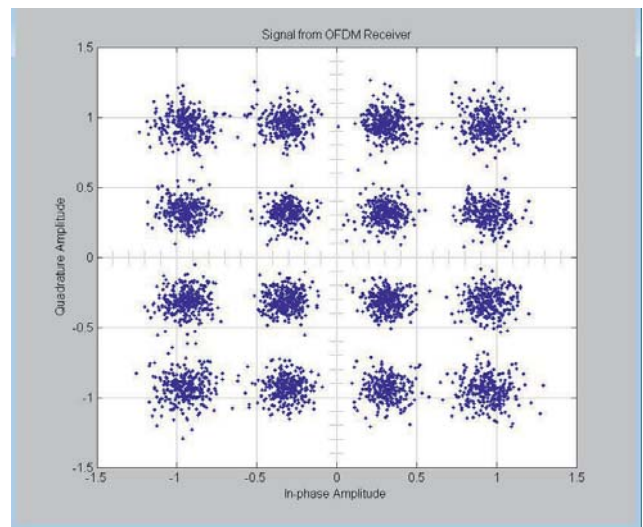


Figure 4. Constellation diagram (16-QAM).

5 Simulation Results

5.1 Gaussian Channel

In our first experiment, we used Gaussian channel with added white noise only. Here it should not be important the use of guard interval, because there is only one main path, without any delays. However slightly different results are possible. Also, pilot carriers and channel estimation introduce error (channel is uniform), so higher C/N is required compared with results obtained without channel

estimation (about 1–3 dB higher). Results are compared with [3], Annex A (informative): Simulated system performance for 8 MHz channels. Simulation duration was set to 1 s and SNR in Gaussian channel was adjusted so that the final BER does not exceed $2 \cdot 10^{-4}$, after Viterbi decoder. According to [3] channel should be QEF (Quasi Error Free) after RS decoder. Results are shown in Table 1 (guard interval 1/4), for our simulation and for system simulated in [3]. At the receiver side, guard interval is removed (first

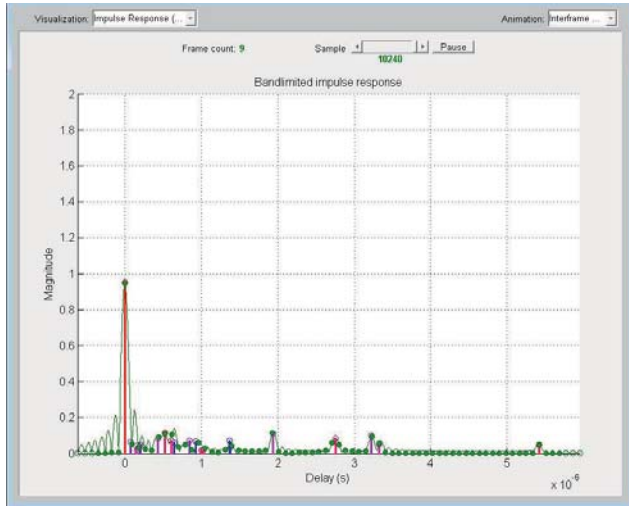


Figure 5. Bandlimited impulse response in Ricean channel (20 delayed paths and 1 main, non-delayed line of sight path).

2048 carriers). Channel estimation is based on [3] (Section 2.8) and pilot signals are transferred in both cases (with and without channel estimation). From the results in Table 1 it can be concluded that our simulation model gives similar results with those achieved in [3], so it can be used for further simulations with added propagation delays.

5.2 Ricean Channel

Ricean fading has been introduced in channel, with parameters somewhat similar to [3], Annex B. Ricean channel is a transmission channel that may have a line-of-sight (direct) component that has usually higher power and several scattered, phase shifted and time delayed, multipath components. Ricean channel is used for fixed reception, different from Rayleigh channel that is used for mobile reception and doesn't have direct path). Ricean fading is described as:

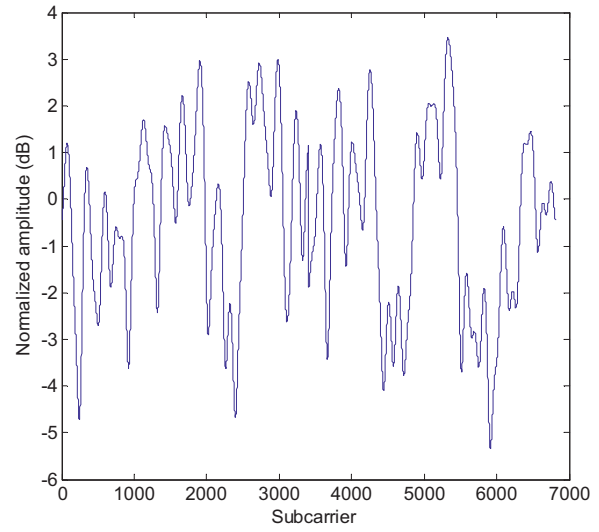
$$y(t) = \frac{\rho_0 \cdot x(t) + \sum_{i=1}^N \rho_i \cdot e^{-j \cdot \theta_i} \cdot x(t - \tau_i)}{\sqrt{\sum_{i=0}^N \rho_i^2}}, \quad (1)$$

where N is number of echoes, θ_i is the phase shift from scattering of the i -th path, ρ_i is the attenuation of the i -th path, τ_i is the relative delay of the i -th path. Case $i = 0$ describes direct path. Ricean factor K (ratio of the power of the direct path to the reflected paths) is given as:

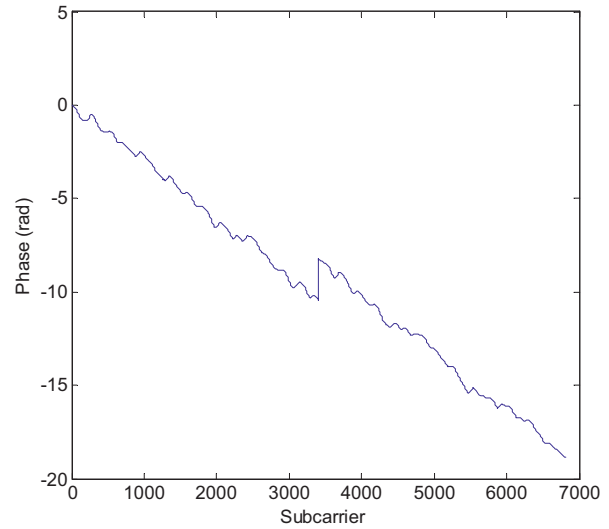
$$K = \frac{\rho_0^2}{\sum_{i=1}^N \rho_i^2}. \quad (2)$$

In our simulation we used $K = 10$ dB (10x). Parameters of the simulated paths are given in Table 2 [3].

Table 3 describes required C/N for our simulated channel and ETSI standard Ricean channel. Our channel uses real channel estimation also (Section 2.8) while ETSI standard



(a)



(b)

Figure 6. Bandlimited impulse response in Ricean channel (20 delayed paths and 1 main, non-delayed line of sight path).

uses 'perfect channel estimation'. This probably means that it is presumed that fading impact was known at the receiver side so it is multiplied with its inverted characteristic (only for fading effect, (5)). In first two simulations zero-forcing (ZF) and minimum mean square error (MMSE) methods were used. ZF inverts the frequency response of the channel. At the receiver side, input has to be multiplied with ZF:

$$\text{ZF} = \frac{H^*}{|H|^2} = \frac{1}{H}, \quad (3)$$

where H is channel estimation based on pilot carriers.

Modulation	Code rate	Our results with channel estimation (MMSE) rate	Our results without channel estimation	ETSI Standard
QPSK	1/2	4.1	2.8	3.5
	2/3	6.1	4.8	5.3
	3/4	6.7	5.5	6.3
	5/6	7.6	6.5	7.3
	7/8	8.2	7.2	7.9
16-QAM	1/2	9.7	8.4	9.3
	2/3	12.2	10.9	11.4
	3/4	13	11.9	12.6
	5/6	14.2	13.0	13.8
	7/8	15.0	13.7	14.4
64-QAM	1/2	14.3	13.1	13.8
	2/3	17.5	16.3	16.7
	3/4	18.8	17.4	18.2
	5/6	20.0	18.7	19.4
	7/8	20.8	19.5	20.2

Table 1. Required C/N (dB), Gaussian channel.

MMSE minimizes the mean square value of the error between the transmitted signal and the output of the equalizer [15]:

$$\text{MMSE} = \frac{H^*}{|H|^2 + \sigma^2}, \quad (4)$$

where H is channel estimation based on pilot carriers and σ^2 variance of the noise (calculated from remaining $8192 - 6817 = 1375$ carriers which don't carry any information). At the receiver side, input has to be multiplied with MMSE.

Ricean channel was simulated firstly by using Matlab 'Ricean Fading' block, but with very high ratio of the line of sight components and corresponding reflected components (K in block was set to 100 000 for all 21 paths; this K is not the same as the K value in (2), which was set to 10). In this way all paths, delays and phases remain constant through all simulation period, imitating Ricean channel described in ETSI standard. Normalized frequency response (mean of amplitudes of all 6817 carriers equals $1 V/\Omega$) used for simulation of the Ricean channel at the receiver input is shown in Figure 6. Because Ricean channel should be time invariant, channel matrix can be calculated from two successive symbols and then every subsequent symbol can be multiplied with the same matrix, imitating fading channel (this also accelerates simulation). Channel matrix was normalized so that mean of all carrier amplitudes equals to 1. Guard interval was set to 1/4 of the useful symbol duration.

i	$\rho_i(\text{Ricean})$	$\rho_i(\text{Rayleigh})$	τ_i (μs)	θ_i (rad)
0	0.953462	–	0	0
1	0.016187	0.053687	1.003019	4.855121
2	0.049635	0.164620	5.422091	3.419109
3	0.114301	0.379093	0.518650	5.864470
4	0.085224	0.282656	2.751772	2.215894
5	0.072647	0.240941	0.602895	3.758058
6	0.017358	0.057568	1.016585	5.430202
7	0.042204	0.139975	0.143556	3.952093
8	0.014467	0.047981	0.153832	1.093586
9	0.051955	0.172315	3.324866	5.775198
10	0.112561	0.373324	1.935570	0.154459
11	0.083017	0.275336	0.429948	5.928383
12	0.098485	0.326639	3.228872	3.053023
13	0.073805	0.244784	0.848831	0.628578
14	0.063414	0.210321	0.073883	2.128544
15	0.048003	0.159207	0.203952	1.099463
16	0.042031	0.139401	0.194207	3.462951
17	0.067413	0.223585	0.924450	3.664773
18	0.032729	0.108549	1.381320	2.833799
19	0.062084	0.205908	0.640512	3.334290
20	0.072913	0.241824	1.368671	0.393889

Table 2. Normalized amplitude (overall power 0 dB), phase and delay values for simulated Ricean and Rayleigh channel.

At the receiver side, guard interval is removed (first 2048 carriers, although it is possible to achieve better results if some minor shift is introduced in guard removal, e.g. 4–30 samples). Simulation duration was set to 1 s and SNR was adjusted so that the final BER will be below $2 \cdot 10^{-4}$ after Viterbi decoder. Numbers in brackets represent minimum achievable BER for our added AWGN $\rightarrow 0$.

It should be also noted that in channel construction TPS carriers had values 0 (in Matlab simulated channel), which means they passed channel only with Gaussian noise and because of that, if they're regarded as useful information, BER could be somewhat worse (up to 0.5 dB for BER $\cdot 2 \cdot 10^{-4}$). Also, zero padding was not taken into channel construction, because we skipped subcarriers 3810–4785. This can also have influence on MMSE channel estimation, because standard deviation was calculated only from Gaussian noise influenced channel in zero padded subcarriers, so it is possible that we have somewhat better results (for

Modulation	Code rate	Our results (ZF method)	Our results (MMSE method)	Our results ('known' channel)	ETSI Standard
QPSK	1/2	8.3	4.9	4.0	4.1
	2/3	9.3	7.2	6.2	6.1
	3/4	9.7	8.1	7.0	7.2
	5/6	10.2	9.3	8.2	8.5
	7/8	10.8	10.1	8.9	9.2
16-QAM	1/2	11.2	10.7	9.5	9.8
	2/3	13.7	13.6	12.3	12.1
	3/4	14.8	14.8	13.2	13.4
	5/6	17.2	17.2	14.6	14.8
	7/8	20.2	20.2	15.4	15.7
64-QAM	1/2	15.5	15.4	14.1	14.3
	2/3	19.6	19.6	17.5	17.3
	3/4	23.1	23.1	18.7	18.9
	5/6	27.5 (0.0006)	27.5 (0.0006)	20.2	20.4
	7/8	30.7 (0.001)	30.7 (0.001)	21.1	21.3

Table 3. Required C/N (dB), Ricean channel, Matlab generated channel matrix.

Modulation	Code rate	Our results (ZF method)	Our results (MMSE method)	Our results ('known' channel)	ETSI Standard
QPSK	1/2	7.5	4.7	3.7	4.1
	2/3	8.7	6.9	5.9	6.1
	3/4	9.1 (*)	7.7	6.7	7.2
	5/6	9.8 (*)	8.8	7.8	8.5
	7/8	10.2	9.6	8.5	9.2
16-QAM	1/2	10.7	10.4	9.2	9.8
	2/3	13.3	13.2	12	12.1
	3/4	14.1	14.1	12.9	13.4
	5/6	15.5	15.5	14.3	14.8
	7/8	16.3	16.3	15	15.7
64-QAM	1/2	15.1	15	13.8	14.3
	2/3	18.5	18.5	17.2	17.3
	3/4	19.7	19.7	18.5	18.9
	5/6	21.2	21.2	19.9	20.4
	7/8	22.1	22	20.7	21.3

Table 4. Required C/N (dB), Ricean channel, signal generator constructed channel matrix.

MMSE method). Phase jump on Figure 6(b) is because of the disregarded zero padded subcarriers, which represent higher frequencies in final OFDM symbol.

In first two simulations, channel fading and noise were calculated using 701 scattered and continual pilots and interpolated points between them (linear interpolation), so

that it would be equal to the number of carriers in one OFDM symbol (6817). In channel compensation block, ZF or MMSE multiplies OFDM symbol, giving reconstructed symbol at its output. In third simulation, inverted characteristic of the 'known' Ricean channel was multiplied with symbol. Final signal in the receiver, after channel estima-

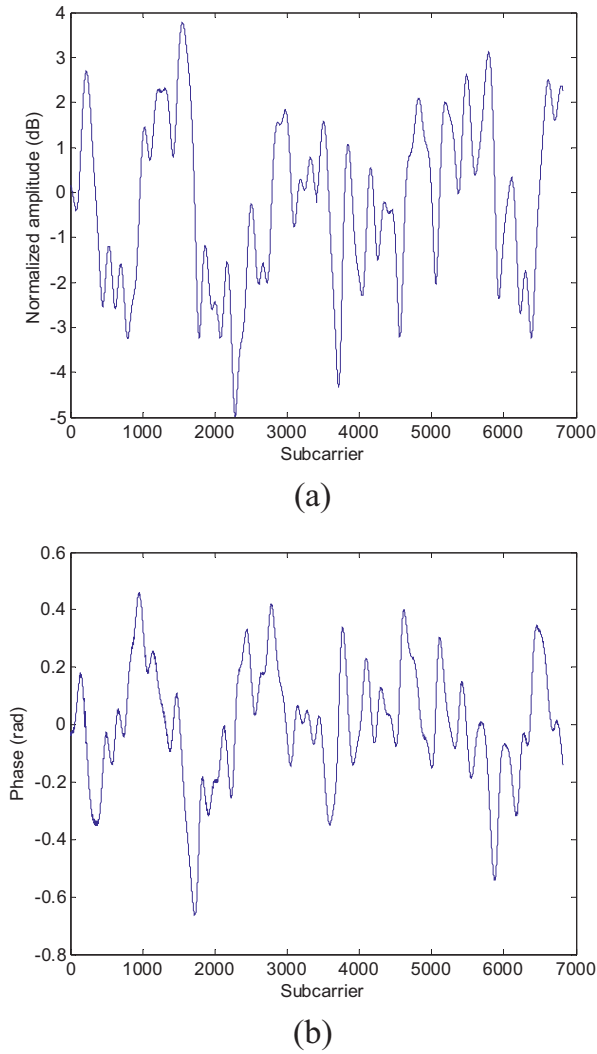


Figure 7. Frequency response ((a) – amplitude, (b) – phase) in simulated Ricean channel, Matlab constructed channel.

tion and compensation, will be:

$$\begin{aligned} \text{input}(f) &= F(F^{-1}(X(f)) \cdot \text{channel}(f)) \\ &\quad + \text{AWGN}(t) \cdot \frac{1}{\text{channel}(f)}, \quad (5) \\ \text{input}(f) &= X(f) + \frac{F(\text{AWGN}(t))}{\text{channel}(f)}. \end{aligned}$$

From (5) it can be seen that for higher degradations in channel, input at the receiver after channel estimation will have worse results and for lower degradations ($\text{channel}(f) \rightarrow 1$) it will have similar results like Gaussian channel. It can be seen that results obtained this way have identical C/N in comparison with ETSI standard (difference is only up to 0.3 dB).

In Table 4 channel was constructed using signal generator constructed channel and then measured its spectral

characteristic in every carrier – both phase and amplitude, Figure 7. Channel matrix was normalized so that mean of all carrier amplitudes equals to 1, but this mean was already very near 1. Guard interval was again set to 1/4 of the useful symbol duration. At the receiver side, guard interval is removed. All three methods described above (ZF, MMSE and ‘perfect channel estimation’) were used and results are shown in Table 4. (*) in Table 4 represents that burst of error bits passed RS decoder and numbers in brackets represent minimum achievable BER for our added AWGN $\rightarrow 0$. Channel noise which was already present (measured by the signal analyzer), before adding our AWGN in Simulink model, was 34.75 dB so it can be ignored. DVB-T/H simulator consists of MXG signal generator with signal creation software (Signal Studio for Digital Video) and EXA signal analyzer with DVB-T/H measurement application.

5.3 Rayleigh channel

Rayleigh fading has been introduced in channel, with parameters similar to [3], Annex B (Table 2). Similar simulations were performed like in section B. Results are presented in Figures 8–9 and Tables 5 and 6, for Matlab and signal generator constructed channels. (*) in Table 5 represents that burst of error bits passed RS decoder and numbers in brackets represent minimum achievable BER for our added AWGN $\rightarrow 0$. For 64-QAM modulation and some FEC values there isn’t any C/N with which BER can be QEF after RS decoder (– in Tables 5 and 6). This means that it is impossible to transfer TS package from transmitter to the receiver, because channel introduced too many uncorrectable errors.

Signal generator constructed channel gave high C/N results or even uncorrectable channel, probably also because of the signal analyzer sensitivity and signal generator characteristics. Also, instruments were deliberately operated without outer synchronization because we wanted to examine behavior in real conditions. Channel noise which was present at the first place was 18 dB, which was under lowest value for some channel modulations and guard values (it can be seen in Table 6, ETSI Standard) so here it cannot be ignored.

From Tables 4 and 6 it can generally be concluded that only robust modulations and FEC redundancies can be used for Rayleigh fading channel (4-QAM and 16-QAM with FEC up to 2/3, with MMSE method). Also, ‘known channel’ gives worse results than MMSE method (where MMSE can repair introduced errors), because of the channel (f) which is highly degraded in Rayleigh channel model (5). Anyway, if C/N is high enough (up to 50 dB, which is the largest observed decline, as shown in Figure 8 (a)), receiver can accurately decode sent TS packet with known channel characteristic. It can be also seen that with our channel sim-

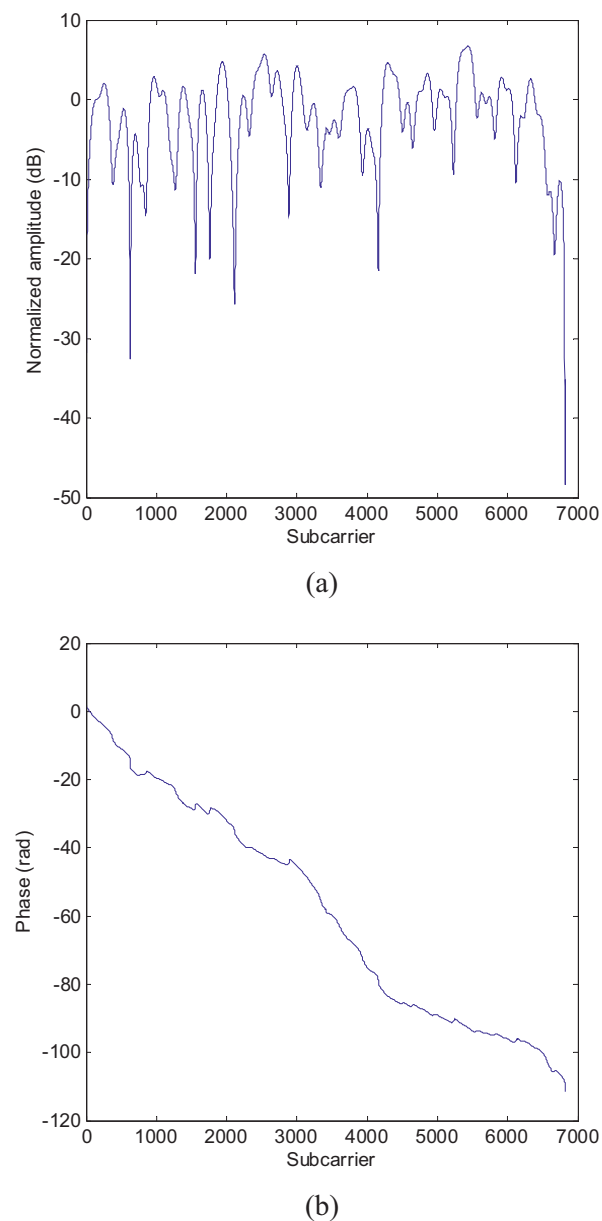


Figure 8. Frequency response ((a) – amplitude, (b) – phase) in simulated Ricean channel, signal generator constructed channel.

ulation C/N values are much higher than those proposed in ETSI standard.

5.4 Real Channel Simulation

Measurements were obtained at 11th floor in our faculty building, a typical indoor signal reception in high buildings in urban zone. Position of the receiver is higher than position of the transmitter. Room has windows that have LOS (Line of Sight) with transmitter. Propagation path is shown

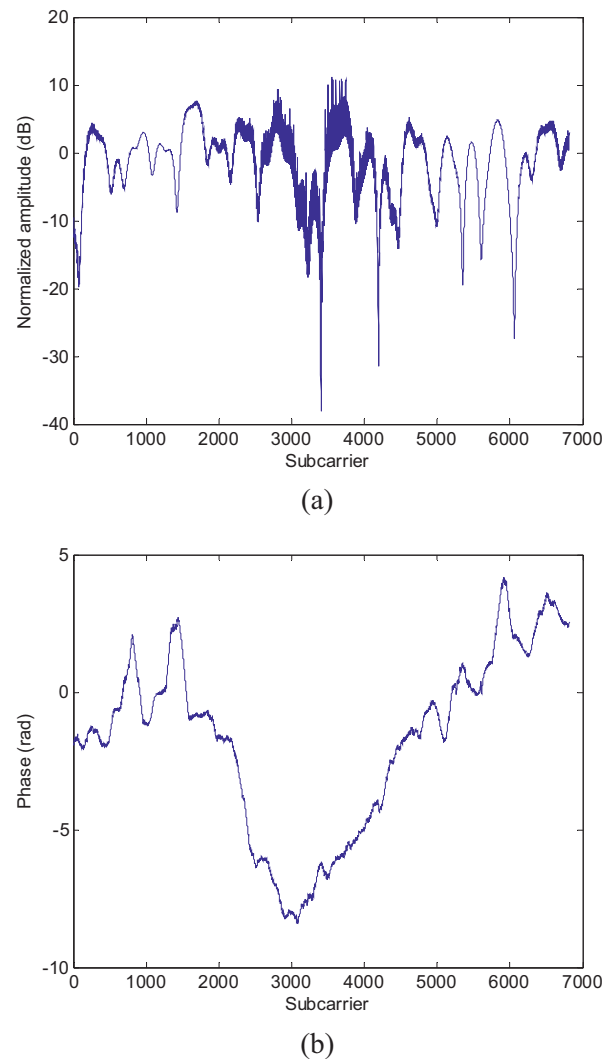


Figure 9. Frequency response ((a) – amplitude, (b) - phase) in simulated Rayleigh channel, Matlab constructed channel.

in Figure 10. Measurements were done in different locations at the relative height of 1.5 m from the floor. We will present only some more important results. Measurement equipment used for indoor measurement was:

- calibrated adjustable dipole antenna, EMCO model 3121C;
- calibrated cable with length of 5m;
- EXA signal analyzer with DVB-T/H measurement application.

We suppose that the channel is time invariant. To estimate real channel characteristics, measured results were averaged 20 times. Dipole antenna is used because it has small directivity as commonly used indoor (portable) antennas. Simulations produced with real channel characteristics have

Modulation	Code rate	Our results (ZF method)	Our results (MMSE method)	Our results (‘known’ channel)	ETSI Standard
QPSK	1/2	27.5	8.5	28.6	5.9
	2/3	38.3	12.8	35.5	9.6
	3/4	38.0	15.1	35.1	12.4
	5/6	42.0	17.9	36.3	15.6
	7/8	43.4	20.6	37.6	17.5
16-QAM	1/2	36.0	16.9	34.5	11.8
	2/3	43.5 (0.0003)	23.7	39.9	15.3
	3/4	44.5 (0.0004)	26.6	40.6	18.1
	5/6	45.0 (0.001)	30.0 (0.0007)	43.3	21.3
	7/8	46.0 (0.0024)	32.0 (0.0022)	45.4	23.6
64-QAM	1/2	42.5 (0.0003)	22.8	38.5	16.4
	2/3	47.0 (0.001)	28.5 (0.001)	43.6	20.3
	3/4	45.0 (0.002)	31.7 (0.002) (*)	44.5	23.0
	5/6	–	–	47.2	26.2
	7/8	–	–	49.0	28.6

Table 5. Required C/N (dB), Rayleigh channel, matlab generated channel matrix.

Modulation	Code rate	Our results (ZF method)	Our results (MMSE method)	Our results (‘known’ channel)	ETSI Standard
QPSK	1/2	26.4	7.8	21.8	5.9
	2/3	34.7	12.6	27.3	9.6
	3/4	34.7	14.7	27.3	12.4
	5/6	36.2	17.7	29.3	15.6
	7/8	36.8	19.9	30.5	17.5
16-QAM	1/2	34.8	16.7	27.0	11.8
	2/3	39.8	24.7	32.3	15.3
	3/4	41.5	28.3	33.1	18.1
	5/6	44.7 (0.0005)	37.3 (0.0005)	35.4	21.3
	7/8	46 (0.0009)	43.1 (0.0009)	37.2	23.6
64-QAM	1/2	43.1 (0.0009)	31.1 (0.0008)	30.7	16.4
	2/3	–	–	36.2	20.3
	3/4	–	–	37.4	23.0
	5/6	–	–	40.4	26.2
	7/8	–	–	41.6	28.6

Table 6. Required C/N (dB), Rayleigh channel, signal generator channel matrix.

upper limitation of maximum achievable C/N. This means that BER cannot be better for C/N values greater than results for channel noise which are measured with signal analyzer. For this reason, adequate channel modeling can be done only in positions where strong received signal exists (e.g. where our added AWGN is much higher than already existing channel noise). Else, hardware limitations prevent BER calculations for wider C/N range. In our measurement in laboratory room the worst measured channel noise (al-

ready present in channel measurement) with signal analyzer was ≈ 23 dB for vertically polarized antenna, Table 7.

Transmitted DVB-T signals have specifications as follows:

- UHF channel 25 ($f_c = 506$ MHz): 64-QAM, FEC 3/4, guard interval 1/4, horizontal polarization;
- UHF channel 48 ($f_c = 690$ MHz): 64-QAM, FEC 3/4, guard interval 1/4, horizontal polarization.

	Channel and polarization	Distance from window [m]	Signal strength [dB μ V/m]	Measured channel noise [dB]
Position 1	25, H polarized antenna	1.5	100.7	32.6
	25, V polarized antenna	1.5	92.8	31.0
Position 2	25, H polarized antenna	2.5	102.2	32.7
	25, V polarized antenna	2.5	85.6	22.8
	48, H polarized antenna	2.5	103.1	31.9
	48, V polarized antenna	2.5	88	23.3

Table 7. Measured results.

	Channel and polarization	ZF method	MMSE method	'known' channel
Position 1	25, H polarized antenna	19.2	19.2	17.8
	25, V polarized antenna	22.2	22.0	20.3
Position 2	25, H polarized antenna	19.5	19.5	18.1
	25, V polarized antenna	35.5 (0.0003)	30.7 (0.0003)	26.9
	48, H polarized antenna	19.0	19.0	17.7
	48, V polarized antenna	39.6 (0.0005)	36.1 (0.0005)	27.8

Table 8. Required C/N (dB) in simulation (produced with existing channel noise and added AWGN in Simulink model).



Figure 10. Frequency response ((a) – amplitude, (b) – phase) in simulated Rayleigh channel, signal generator constructed channel.

DVB-T indoor reception has been measured both in horizontal and vertical polarization plane. Results obtained at locations that are 1.5 m and 2.5 m away from window are shown in Figures 11–12 and Table 7.

Signal analyzer has also capability to measure channel frequency response (amplitude and phase) which is then used in our DVB-T system model. It is possible to model the behavior of DVB-T system in real channels (in our case that is indoor signal reception in high buildings). Described method is very simple and efficient, especially for educational purposes, but with some limitations.

In Sections 5.1 and 5.2, we proved that our simulation gives similar results with ETSI standard for all cases with 'known' channel. So, we proved the regularity of our system model written in Simulink. Now, we tested the behavior of DVB-T system in measured channels. Channels should be QEF (Quasi Error Free) after RS decoder, if the calculated BER does not exceed $2 \cdot 10^{-4}$ after Viterbi decoder. Table 8 presents minimum required added AWGN to achieve $BER < 2 \cdot 10^{-4}$, when possible, after Viterbi decoder, except for Position 2, vertically polarized antenna (numbers are in italic). Here is C/N in fact minimal C/N which does not influence on the already existing channel noise (which is 23 dB from Table 7). Numbers in brackets represent minimum BER which is present even if our added AWGN $\rightarrow 0$.

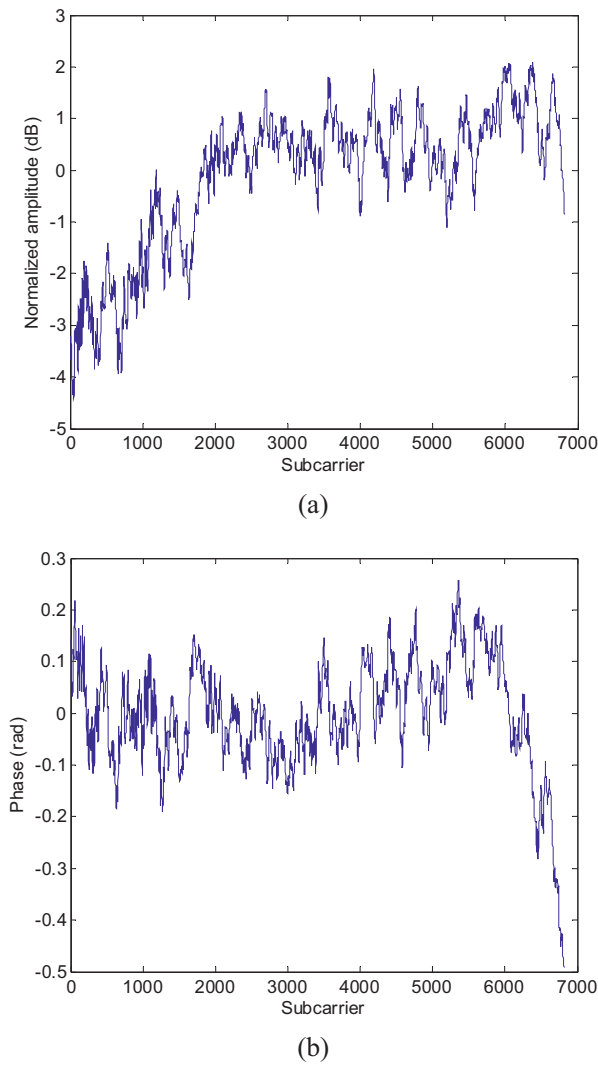


Figure 11. Measured distance from transmitter to receiver is ≈ 988 m.

5.5 Discussion of the Results

In Sections 5.2–5.4 we compared several channel types (ETSI Ricean, ETSI Rayleigh and real channels measured in laboratory room in high building) and calculated required C/N to obtain QEF reception. In Ricean and Gaussian channel, our simulation gives similar results with those in ETSI standard. Exception is Rayleigh channel, especially when it was constructed with MXG signal generator and signal creation software. This means that model can be used for other real channel simulations, like the one described in Section 5.4. This was, in fact, calibration process of our Simulink model or first step in evaluation of DVB-T system in real channels. Firstly, MMSE method gives significantly better results when lower C/N values are needed (this means, for more robust modulation schemes) and equal results with higher C/N. This is in accordance with (4) because when $C/N \rightarrow \infty$ MMSE equalizer becomes identi-

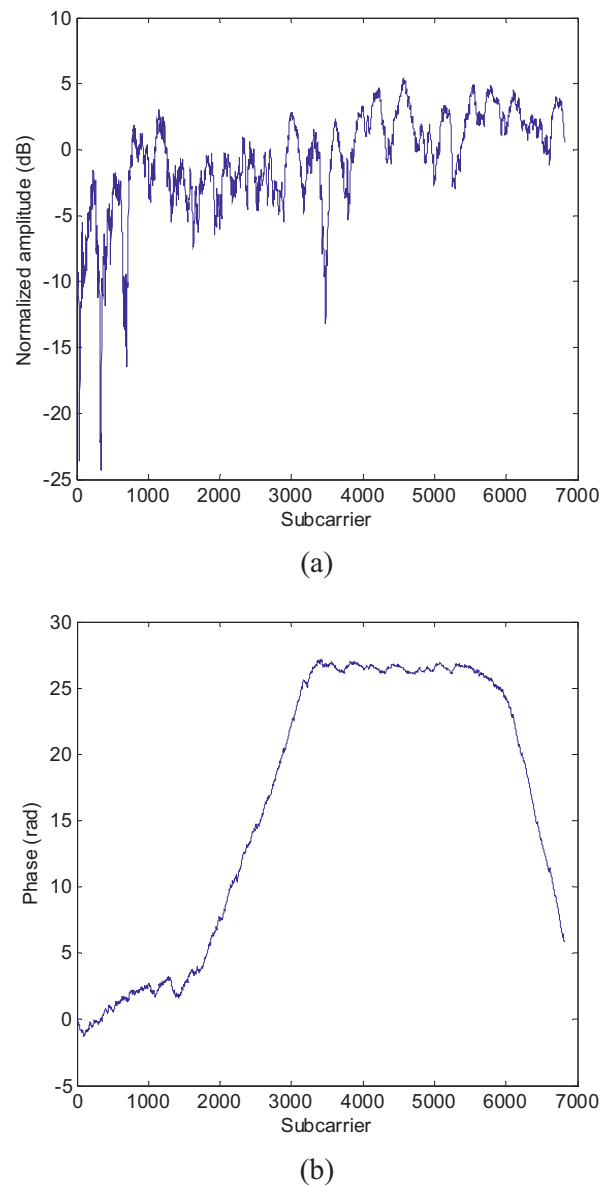


Figure 12. Frequency response ((a) – amplitude, (b) – phase) in real channel UHF 25 (horizontal dipole antenna).

cal to ZF equalizer. In fact, MMSE will be useful only with QPSK and eventually 16-QAM. In section D where we tested real channel, results are the same for ZF and MMSE method. When comparing position 1 and 2, it can be seen that much better results are obtained when we had situation similar like LOS (Line of Sight) in position 1. Here we could reconstruct signal (with $BER < 2 \cdot 10^{-4}$) even with vertically polarized antenna, because of the signal strength. In position 2, only with horizontally polarized antenna we could achieve $BER < 2 \cdot 10^{-4}$ after Viterbi decoder. Anyway, with vertically polarized antenna again we didn't have errors after RS decoder even with $BER 5 \cdot 10^{-4}$, which means that even here it is possible to have normal signal reception. When comparing results for 25 and 48 channel,

we can see that results are pretty much the same. In all situations and positions, when we used perfect channel estimation ('known channel'), we could achieve $BER < 2 \cdot 10^{-4}$, but this cannot be done in real situations where channel frequency response is unknown at the first place.

It can be also seen that for horizontally polarized antenna, required C/N is in practice similar to the C/N in simulated Ricean channel, Tables 3 and 4 (64-QAM with FEC 3/4). For vertically polarized antenna at position 2, C/N is much worse, but better than simulated Rayleigh channel (constructed in Matlab, Table 5). Anyway it can be compared with Rayleigh because there are probably many echoes with not direct signal path, like in Rayleigh channel.

6 Conclusion

In this paper we presented results of simulated and real channel characteristics in DVB-T system. We tested Gaussian, Ricean and Rayleigh channels as defined in ETSI standard and channel with real measured characteristics. Results show that channel models give similar results as results given in ETSI EN 300 744 for Gaussian channel (0.9 dB maximum difference for channel simulation without channel estimation) and Ricean channel (up to 0.3 dB for 'known channel' estimation). Rayleigh model in our implementation requires much higher C/N values than those proposed in ETSI standard. It means that high fades in frequency characteristic have major impact on quality of reception. In such case only robust modulations will have stable reception. Simulated channel is then compared with real measured channel (with system parameters as in Croatian DVB-T network). C/N measured results for horizontally polarized antenna are similar to ETSI defined Ricean channel with $K = 10$.

The proposed simulation model can be extended by new coding techniques and signal detection methods, as well as for the DVB-T2 simulation model.

Acknowledgments

The work described in this paper was conducted under the research projects: "Picture Quality Management in Digital Video Broadcasting" (036-0361630-1635) supported by the Ministry of Science, Education and Sports of the Republic of Croatia.

References

- [1] J. G. Proakis, M. Salehi, "Fundamentals of Communication Systems", Prentice-Hall, 2005.
- [2] U. Reimers, Digital Video Broadcasting, Springer, 2001.
- [3] ETSI EN 300 744 (V1.6.1), Digital Video Broadcasting (DVB); Framing structure, channel coding and modulation for digital terrestrial television, September 2008.
- [4] ISO/IEC 13818-1, Information Technology – Generic Coding of moving pictures and associated audio – Part 1: Systems, 1996.
- [5] ETSI TS 101 154 (V1.8.1), Digital Video Broadcasting (DVB); Specification for the use of Video and Audio Coding in Broadcasting Applications based on the MPEG-2 Transport Stream, July 2007.
- [6] J. H. Stott, "The how and why of COFDM", EBU technical Review, No. 278 (1998).
- [7] O. Hüttl, T. Kratochvíl, "DVB-T channel coding implementation in Matlab", Mezinárodní konference Technical Computing Prague, Inproceedings of MATLAB conference, 2009.
- [8] R. Schramm, "DVB-T – C/N values for portable single and diversity reception", EBU technical review, No. 298 (2004).
- [9] ISO/IEC 13818-2, Information Technology – Generic Coding of moving pictures and associated audio – Part 2: Video, 1996.
- [10] ITU-T Recommendation H.264 / ISO/IEC 14496-10, Information technology – Coding of audio-visual objects – Part 10: Advanced Video Coding, 2005.
- [11] SMPTE 421M, VC-1 Compressed Video Bitstream Format and Decoding Process.
- [12] ISO/IEC 13818-3, Information technology – Generic coding of moving picture and associated audio information – Part 3: Audio, 1996.
- [13] ISO/IEC 13818-7, Information Technology – Generic coding of moving pictures and audio – Part 7: Advanced Audio Coding, AAC, 1997.
- [14] ETSI TS 102 366, Digital Audio Compression (AC-3, Enhanced AC-3) Standard, 2007.
- [15] K. Fazel, S. Kaiser, "Multi-Carrier and Spread Spectrum Systems", Second Edition, Wiley, 2008.